Tropical cyclones and the flood hydrology of Puerto Rico

James A. Smith,[1] Paula Sturdevant-Rees,[2] Mary Lynn Baeck,[1] and Matthew C. Larsen[3]

Received 27 July 2004; revised 20 December 2004; accepted 17 January 2005; published 29 June 2005.

[1] Some of the largest unit discharge flood peaks in the stream gaging records of the U.S. Geological Survey (USGS) have occurred in Puerto Rico. Many of these flood peaks are associated with tropical cyclones. Hurricane Georges, which passed directly over the island on 21–22 September 1998, produced record flood peaks at numerous USGS stations in Puerto Rico. The hydrology and hydrometeorology of extreme flood response in Puerto Rico are examined through analyses of rainfall, based on Weather Surveillance Radar–1988 Doppler (WSR-88D) radar reflectivity observations and USGS rain gage observations and discharge from USGS stream gaging stations. Peak rainfall accumulations of more than 700 mm occurred in the central mountain region of the island. The largest unit discharge flood peaks, however, were located in the eastern portion of the island in areas with smaller storm total rainfall accumulations but markedly larger rainfall rates at 5–60 min timescale. Orographic precipitation mechanisms played an important role in rainfall distribution over the island of Puerto Rico. Amplification of rainfall accumulations was associated with areas of upslope motion. Elevated low-level cloud water content in regions of upslope motion played an important role in the maximum rainfall accumulations in the central mountain region of Puerto Rico. The largest unit discharge flood peaks, however, were produced by a decaying eye wall mesovortex, which resulted in a 30–45 min period of extreme rainfall rates over the eastern portion of the island. This storm element was responsible for the record flood peak of the Río Grande de Lóiza. The role of terrain in development and evolution of the eye wall mesovortex is unclear but is of fundamental importance for assessing extreme flood response from the storm. Hydrologic response is examined through analyses of rainfall and discharge from five pairs of drainage basins, extending from east to west over the island. These analyses point to the importance of short-term rainfall rates for extreme flood response. The hydrologic response of Puerto Rico is compared with two other extreme flood environments, the central Appalachians and Edwards Plateau of Texas. These analyses suggest that the high rainfall environment of Puerto Rico is linked to the development of a hydraulically efficient drainage system.

Citation: Smith, J. A., P. Sturdevant-Rees, M. L. Baeck, and M. C. Larsen (2005), Tropical cyclones and the flood hydrology of Puerto Rico, *Water Resour. Res.*, *41*, W06020, doi:10.1029/2004WR003530.

1. Introduction

[2] The flood hydrology of Puerto Rico is of special interest because of the high frequency of extreme "unit discharge" flood peaks relative to other locations in the United States [*O'Connor and Costa*, 2004]. Tropical cyclones play a central role in the hydrology of extreme floods in Puerto Rico [see *Scatena and Larsen*, 1991; *Larsen and Simon*, 1993; *Larsen and Torres-Sanchez*, 1998] and many of the record flood peak measurements in Puerto Rico were associated with tropical cyclones, most notably Hurricane Donna (6 September 1960 [see *Barnes and Bogart*, 1961]), Hurricane Hortense (10 September 1996 [see *Torres-Sierra*, 1997]) and Hurricane Georges (21–22 September 1998 [see *Larsen and Santiago-Román*, 2001; *U.S. Geological Survey*, 1999]). The principal topics of this paper are the hydrometeorological and hydrologic controls of extreme flood response in Puerto Rico (see Figure 1 for location map) for Hurricane Georges.

[3] *Costa* [1987] examined the largest flood peaks in the conterminous United States at basin scales smaller than 400 km^2 and found that these events occurred in arid to semiarid environments and resulted from an "optimal combination of basin morphology, physiography and storm intensity." The highest frequency of extreme flood peaks in small basins within the conterminous United States is centered in the Edwards Plateau of Texas [*Costa*, 1987; *Baker*, 1977; *Smith et al.*, 2000; *Michaud et al.*, 2001; *Osterkamp and Friedman*, 2000; *Enzel et al.*, 1993]. Costa's envelope curve of 12 flood peaks (Figure 2) contains three events from the Edwards Plateau. The envelope curve of flood peaks in Puerto Rico from Hurricane Georges (Figure 2) is comparable to Costa's envelope curve for the conterminous United States. The

[1]Department of Civil and Environmental Engineering, Princeton University, Princeton, New Jersey, USA.
[2]Department of Civil and Environmental Engineering, University of Massachusetts, Amherst, Massachusetts, USA.
[3]U.S. Geological Survey, Reston, Virginia, USA.

0043-1397/05/2004WR003530

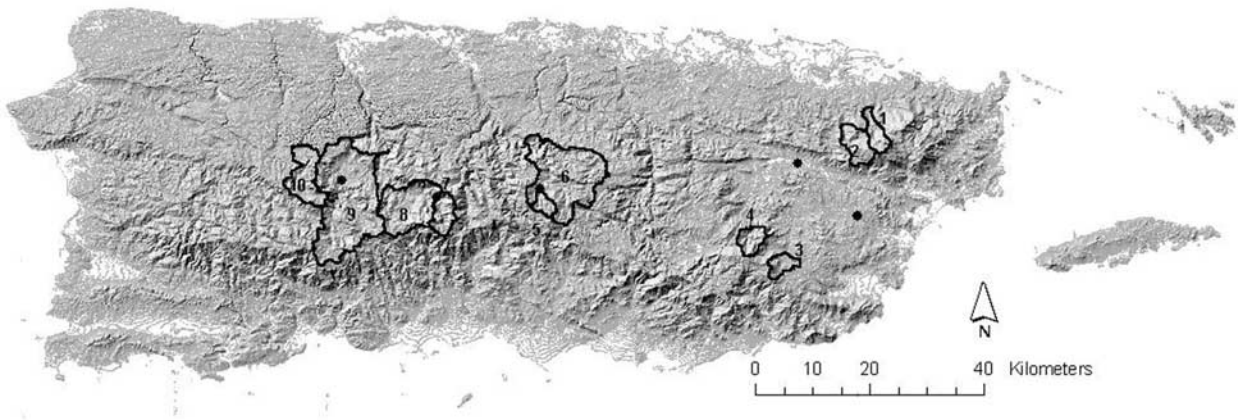

Figure 1. Location map for Puerto Rico study region with shaded relief representation of topography as background map. Paired drainage basins are, from east to west, (1) Río Canóvanas and (2) Río Grande el Verde; (3) Río Grande de Lóiza and (4) Río Turabo; (5) Río Orocovis and (6) Río Grande de Manatí; (7) Río Saliente and (8) Río Caonillas; and (9) Río Grande de Arecibo and (10) Río Tanamá. Rain gages (circles) are, from east to west, Río Humacao, Río Gurabo, Río Orocovis, Río Saliente, and Río Grande de Arecibo.

estimated flood peak for the Río Grande de Lóiza exceeded the U.S. envelope curve at 15 km^2 scale (see section 3 for additional discussion of this estimated peak).

[4] Given that tropical cyclones play a prominent role in the extreme flood response of Puerto Rico, what are the characteristics of rainfall structure in space and time that control flood peak response? We examine this question through analyses of the spatial and temporal variability of rainfall from Hurricane Georges and the associated hydrologic response. The perspective for examining space-time variability of rainfall focuses on structural organization of tropical cyclone rainfall [see *Marks*, 1985; *Marks and Houze*, 1987; *Bender*, 1997; *Molinari et al.*, 1999; *Cecil et al.*, 2002], storm motion and magnitudes of rainfall rates. Marked changes to storm structure were associated with passage of the storm over Puerto Rico [see *Geerts et al.*, 2000; *Bender et al.*, 1987; *Smith and Smith*, 1995]. As illustrated in section 2, modifications of eye wall convection and rainband structure with the passage of Georges over Puerto Rico are of fundamental importance for space-time variability of rainfall. Orographic amplification of rainfall played an important role in flood response to Hurricane Georges, as well as for many other tropical cyclones [*Geerts et al.*, 2000; *Scatena and Larsen*, 1991; *Sturdevant-Rees et al.*, 2001].

[5] Of particular importance for extreme flood response in Puerto Rico during Hurricane Georges was the development and evolution of an eye wall mesovortex (compare with analyses of Hurricane Danny by *Blackwell* [2000]). This element of the storm was responsible for the record flood peaks over the eastern portion of the island.

[6] To examine the contrasting hydrologic response over the island, five sets of paired basins (Figure 1), extending from west to east across Puerto Rico, are used for hydrologic analyses. This design makes it possible to examine flood response in terms of the pronounced contrasts in rainfall distribution from the eastern to the western end of the island. Analyses of hydrologic response are based on

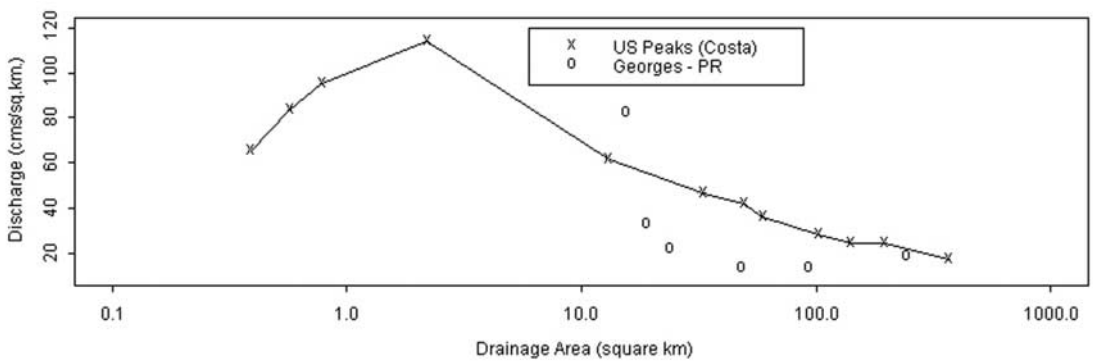

Figure 2. Envelope curve of flood peaks for the United States (data from *Costa* [1987]). Peaks are denoted by crosses, and selected peaks from Hurricane Georges in Puerto Rico are denoted by circles. Flood peaks are expressed as a unit discharge (in m^3 s^{-1} km^{-2}), i.e., peak discharge (in m^3 s^{-1}) divided by drainage area (in km^2).

rain gage, radar and discharge observations for the storm. Rainfall analyses utilize 15 min rain gage observations from a network maintained by the U.S. Geological Survey (USGS) and radar reflectivity observations from the San Juan Weather Surveillance Radar–1988 Doppler (WSR-88D) radar. ''Unit values'' discharge observations at 5–15 min timescale from USGS stream gaging stations are used for analyses of hydrologic response.

[7] Extreme flood response in Puerto Rico is compared to extreme flood response in two other extreme flood environments of the United States, the Edwards Plateau of Texas and the central Appalachian region. We compare flood response in these three regions through analyses of the geomorphological instantaneous unit hydrograph (GIUH) [see *Rodriguez-Iturbe and Rinaldo*, 1997] of the Río Grande de Manatí basin in Puerto Rico, Seco Creek in the Edwards Plateau of Texas [*Baker*, 1977; *Costa*, 1987; *Smith et al.*, 2000] and the Rapidan River basin along the eastern margin of the central Appalachian region [*Smith et al.*, 1996; *Giannoni et al.*, 2003]. Derivation of the GIUH for each basin is based on hydrologic model analyses for flood events each with flood peaks in the 10–20 $m^3\ s^{-1}\ km^{-2}$ range at 100 km^2 scale. The Rapidan River flood peak in the central Appalachians has a return interval greater than 1000 years, the Seco Creek flood peak in the Edwards Plateau has a return interval between 50 and 100 years and the Puerto Rico peak has a return interval in the range of 10–50 years.

[8] Contents of the sections are as follows: Hydrometeorological analyses of Hurricane Georges, including analyses of temporal and spatial variation of rainfall, are presented in section 2. Hydrologic analyses of flood response are presented in section 3. A summary and conclusions are given in section 4.

2. Hydrometeorological Analyses of Hurricane Georges

[9] Hydrometeorological analyses of Hurricane Georges are based on volume scan radar reflectivity observations from the San Juan WSR-88D radar (Figure 1) and rain gage observations from five stations in the USGS rain gage network in Puerto Rico (Figure 1). The evolving structure of rainfall fields over Puerto Rico is examined with the objective of characterizing the space-time variability of extreme flood-producing storms.

[10] Hurricane Georges moved from east to west over Puerto Rico at a mean speed of 21 km h^{-1} (Figures 3a–3h). The 190 km path over the island took 9 hours (from 2120 UTC on 21 September to 0620 UTC on 22 September) and the period of rainfall over the island was approximately 24 hours (from 1930 UTC on 21 September to 2000 UTC on 22 September). The eye of the storm passed directly over the island and storm motion oscillated slightly from northwest, as it reached the island, to west-southwest, as it exited the western end of the island. Storm speed did not vary markedly as the system passed over Puerto Rico. Hurricane Georges weakened as it made landfall, with minimum sea level pressure increasing from 970 to 978 hPa during passage over the island. Minimum sea level pressure decreased to 962 hPa with passage over the Mona Passage between Puerto Rico and the Dominican Republic. The low-reflectivity region of the eye was more than 1000 km^2 in size both on entering the island (Figure 3b) and after exiting the island (Figure 3g).

[11] The frequency with which a tropical cyclone passes directly over Puerto Rico is small [*Scatena and Larsen*, 1991]. The last hurricane to track over the island was San Ciprian in September 1932. Tropical cyclones are rare events, especially those like Hurricane Georges which track directly over the island, and Puerto Rico is a high-rainfall environment even in the absence of tropical cyclones. Annual rainfall ranges from greater than 4000 mm in the eastern mountains to 1000–1500 mm in coastal regions [*Calvesbert*, 1970].

[12] The structure of rainfall fields in Hurricane Georges is examined in terms of the conceptual model of a hurricane presented by *Molinari et al.* [1999] (see also *Cecil et al.* [2002] and *Willoughby et al.* [1984]). In this model, the structure of rainfall within a hurricane is represented by (1) the eye wall region, (2) the inner rainband region and (3) the outer rainband region (the three regions are best represented in Figure 3g). The eye wall is the approximately circular region of precipitation surrounding the circulation center. Adjacent to the eye wall is the inner rainband region, which extends approximately 100 km from the eye. It is often bounded by a precipitation free area adjacent to outer rainbands. The outer rainband region begins approximately 150 km from the cyclone center. *Molinari et al.* [1999] show large contrasts in convective intensity, as reflected in cloud-to-ground (CG) lightning strikes, between the inner core region, consisting of the eye wall and inner rainbands, and outer rainband region of hurricanes. The more convectively active outer rainbands contain the large majority of CG strikes.

[13] Hurricane Georges, like many tropical cyclones [see *Bender*, 1997, and references therein], exhibited an asymmetric rainfall structure around the eye throughout much of the life cycle of the storm. At 1923 UTC (Figure 3a) on 21 September, the eye of Hurricane Georges, which was was approximately 1000 km^2 in area, was less than 50 km from the coastline. On the eastern portion of the island rainfall began at approximately 1930 UTC. At 1923 UTC, the reflectivity structure of the storm exhibited a pronounced asymmetry with more extensive development in the southern and eastern sectors of the storm This pattern of asymmetry persisted throughout much of the life cycle of the storm. Rainbands developed in the southeastern sector of the storm and passed from south to north over the island. Throughout the life cycle of Hurricane Georges over Puerto Rico, the ''upslope'' portion of the storm was located on the south (or southeast) side of the mountains.

[14] The eye of Georges reached the eastern end of the island at 2117 UTC (Figure 3b) and was still structured as a near-circular, low-reflectivity region. A thin inner core rainband extended from north-to-south over the island, passing through the location of the San Juan WSR-88D radar. This band was responsible for the first pulse of high rainfall rates in the eastern and central portions of the island (see Figure 4). During passage of Hurricane Georges over Puerto Rico, the eye region filled rapidly and eye wall convection was influenced by interactions with the terrain of the island (see *Houze* [1993] for a discussion of orographic convection).

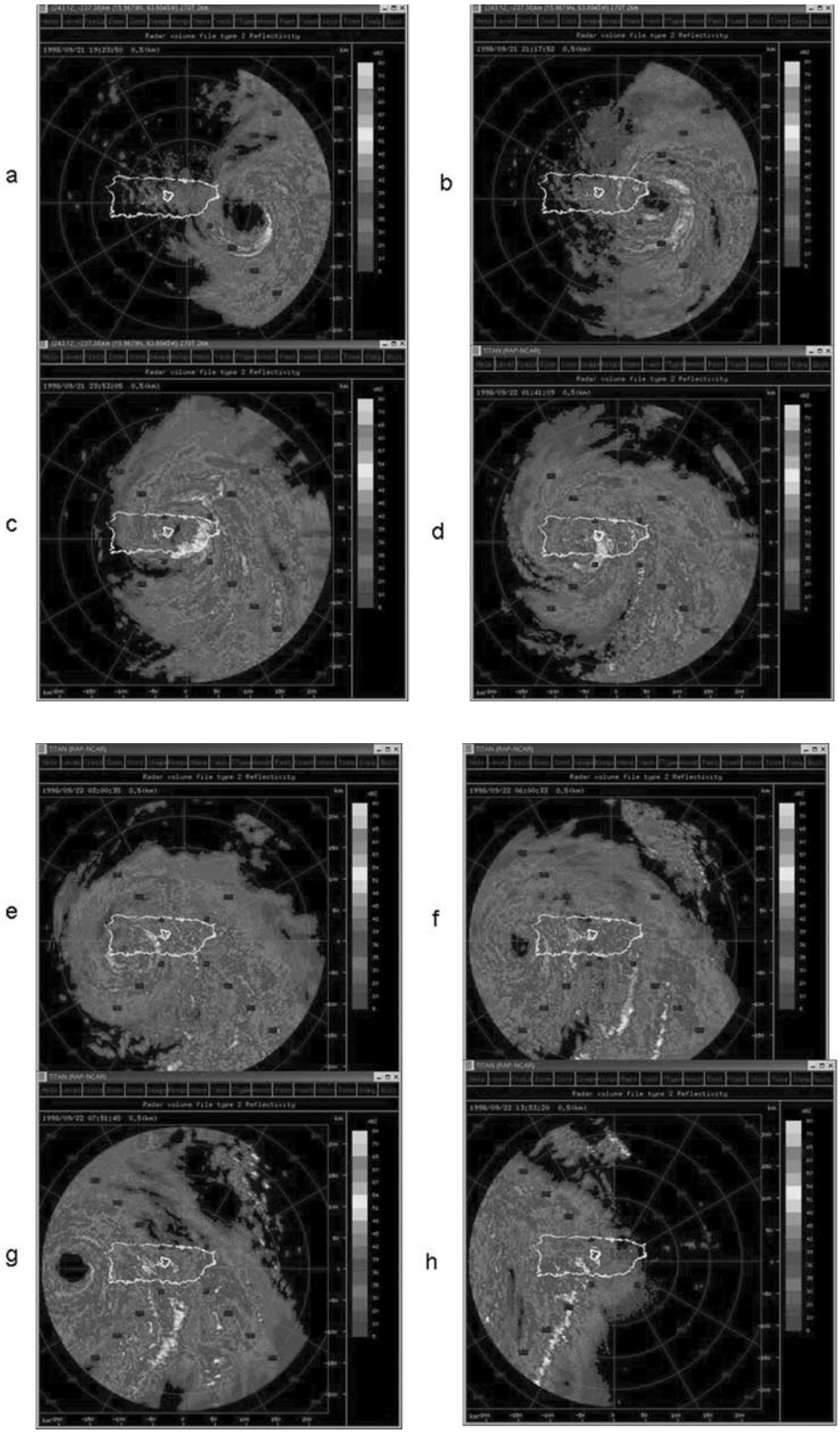

Figure 3. Reflectivity images from the San Juan, Puerto Rico, WSR-88D (lowest elevation angle) for 21 September 1998 at (a) 1923 UTC (b) 2117 UTC, and (c) 2353 UTC and for 22 September 1998 at (d) 0141 UTC (e) 0300 UTC, (f) 0600 UTC, (g) 0751 UTC and (h) 1353 UTC. Puerto Rico is outlined in yellow and the Río Grande de Manatí basin boundary is outlined in white. See color version of this figure at back of this issue.

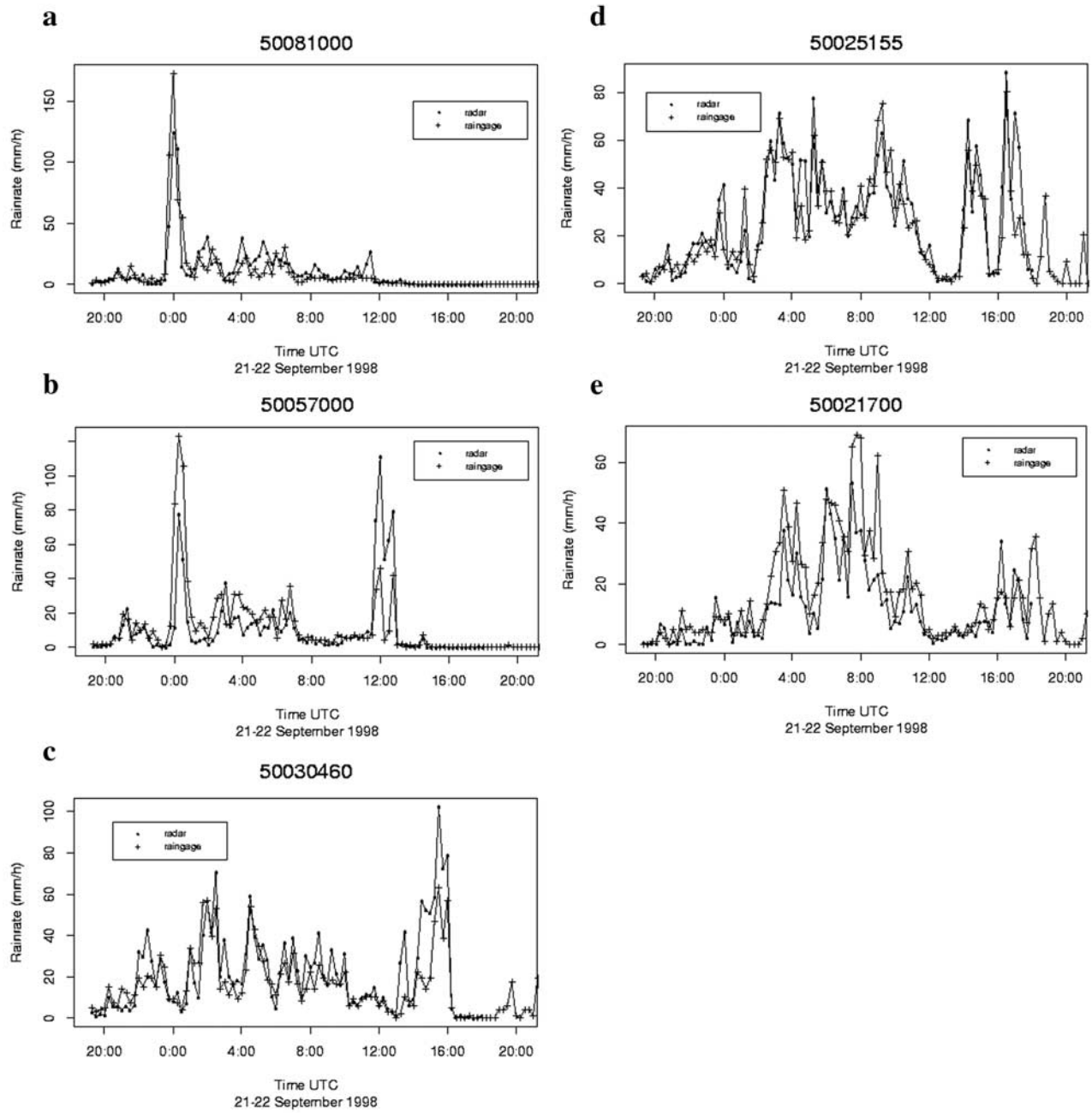

Figure 4. Time series of rain gage and radar rainfall estimates at 15 min time intervals for the (a) Río Humacao (USGS identification number (ID) 50081000), (b) Río Gurabo (USGS ID 50057000), (c) Río Orocovis (USGS ID 50030460), (d) Río Saliente (USGS ID 50025155), and (e) Río Grande de Arecibo (USGS ID 50021700) gages. Radar rainfall estimates were derived using the tropical Z-R relationship (see text for additional details).

[15] The largest rainfall rates from the storm occurred on the eastern portion of the island during a period of less than 1 hour, beginning at approximately 2345 UTC on 21 September. Eyewall convection intensified on its southern side as the eye passed over the eastern margin of the island, resulting in a high-reflectivity region along the southeastern and eastern portion of the island at 2353 UTC (Figure 3c). Peak flood response in the eastern catchments of Puerto Rico (see section 3) was associated with this element of the storm. It produced the record peak discharge for the Río Grande de Lóiza (Figure 2) (see additional discussion in section 3).

[16] The largest rainfall accumulations from the storm occurred in the central mountains of the island and the largest rainfall rates contributing to these peak accumulations were associated with eye wall convection and inner core rainbands (Figures 3d and 3e). During the period of peak rainfall rates over the central mountains (Figures 3d and 3e at 0141 and 0300 UTC), eye wall convection developed over ocean south of the island and wrapped up to the mountain barrier.

[17] Heavy rain fell over the western portion of Puerto Rico for 12 hours after the eye of the storm exited Puerto

Rico at 0600 UTC. As the eye exited the island (Figure 3f), north-south oriented rainbands were producing heavy rainfall (rain rates greater than 25 mm h^{-1}) over the island. Flood response in the western portion of the island (including the Arecibo and Tanamá basins discussed in the following section) [see also *Torres-Sierra*, 2002] resulted from rainband rainfall which developed in the southeastern sector of the storm and intensified over Puerto Rico in north-south oriented regions of embedded convection (Figures 3g and 3h).

[18] Rainfall rate observations at 15 min timescale from five locations in Puerto Rico (Figures 4a–4e) illustrate the time history of flood-producing rainfall over the island. Each of the five locations coincides with the location of a USGS rain gage (Figure 1). Radar rainfall estimates for the 1 km bin containing the rain gage have been paired with the rain gage observations. Radar rainfall estimates were computed using the "tropical" Z-R relationship, $Z = 250\ R^{1.2}$ [*Fulton et al.*, 1998]. For the time series plots, rainfall rate estimates were aggregated from the 5–6 min timescale of the radar volume scan to a regular 15 min time interval.

[19] Peak rainfall rates at Río Humacao (USGS identification number (ID) 50081000) (Figure 1) near the eastern end of Puerto Rico reached 160 mm h^{-1} at 15 min timescale (Figure 4a). Large rainfall rates on the eastern portion of the island, as reflected in the Río Humacao observations, were associated with explosive growth in low-level reflectivity in the eye wall portion of the storm (see Figure 3c and discussion of vertical storm structure below). The storm total rainfall at Río Humacao of 232 mm was largely associated with extreme rainfall rates from eye wall convection during a 1 hour period centered at 0000 UTC on 22 September. The tropical Z-R relationship underestimates peak rainfall rates but slightly overestimates subsequent rainfall with a storm total of 266 mm. The 232 mm accumulation at the Río Humacao station may be an underestimation. Tipping bucket rain gages tend to underestimate rainfall rate as intensity approaches 50 mm h^{-1} [*Barry*, 1992].

[20] The Río Gurabo (USGS ID 50057000) (Figure 1) observations (Figure 4b) show somewhat lower peak rainfall rates (100–110 mm h^{-1}) than for Río Humacao, but larger contributions to storm total accumulation from subsequent rainbands. The storm total accumulation of 307 mm was produced by eye wall convection centered at 0015 UTC on 22 September (Figure 3c), a 5 hour period (0130 to 0630) of 20–40 mm h^{-1} rain rates from inner rainbands (Figures 3c–3g) and a final period of outer rainband rainfall centered at 1200 UTC. The Río Gurabo observations reflect the rainfall distribution in low-elevation regions of the Río Grande de Lóiza basin (elevation of the gage is 42 m above sea level). Rain gage observations are not available at high-elevation regions of the basin. These regions experienced the largest storm total accumulations and were responsible for the record peak discharge from the Río Grande de Lóiza.

[21] The properties of radar rainfall estimates vary systematically with storm structure, as illustrated in the Río Gurabo analyses (Figure 4b). The most important element of these analyses is the overestimation of rain rate in the outer rainband region of the storm, using the tropical Z-R relationship. For the final period of heavy rainfall around 1200 UTC from outer rainbands, radar rainfall estimates for Río Garabo using the tropical Z-R equation are more than 50% larger than rain gage observations. This feature is characteristic of gage-radar intercomparisons over much of the island (see Figures 4c–4e). Overestimation of outer rainband rainfall by the tropical Z-R relationship is consistent with the conclusions of *Molinari et al.* [1999] and *Cecil et al.* [2002] that the outer rainband region of hurricanes is the most convectively active portion of the hurricane. For both of the eastern Puerto Rico rain gages (Figures 4a and 4b) there is a pronounced underestimation of rain rates (from radar) for the period of intense eye wall convection. It is argued below, based on the evolution of vertical structure of this storm element, that vertical motion plays an important role in underestimation of rain rate for this element of the storm [see also *Lee*, 1988; *Jorgensen et al.*, 1985].

[22] The Río Orocovis rain gage (USGS ID 50030460)in the central mountain region of the island (Figure 1) reported markedly larger rainfall accumulation (401 mm) than the eastern gages, but smaller peak rainfall rates (65 mm h^{-1}) (see Figure 4c). The rain gage storm total accumulation of 401 mm was approximately 20% less than the storm total rainfall accumulation from radar. Flood peaks at Río Orocovis and the downstream Río Grande de Manatí gage (Figure 5c) were produced by rainfall from the inner core region of the storm, principally embedded convection which formed over ocean south of the island and wrapped up to the central highlands. Although the peak rainfall rates in the Río Grande de Manatí basin were smaller than those in the eastern portion of the island, it will be seen in the following section, that flood response is still strongly controlled by peak rainfall rates.

[23] The rain gage collocated with the Río Saliente stream gage (USGS ID 50025155) (Figure 1) recorded 532 mm of rainfall. There was excellent agreement in temporal pattern of rain rates between gage and radar (Figure 4d). The storm total rainfall from radar rainfall estimates using the tropical Z-R relationship was 617 mm. Peak 15 min rainfall rates of 80 mm h^{-1} were recorded at the Río Saliente rain gage. The overestimation of storm total rainfall at Río Saliente is due to overestimation of rainfall for the outer rainband convection that passed over the region from 13–18 UTC. As noted above, this feature is characteristic of gage-radar intercomparisons for Hurricane Georges.

[24] The peak in Arecibo rainfall rates (USGS ID 50021700) (Figure 1) occurred at 0800 UTC (see Figure 4e) and was produced by rainbands. Río Tanamá and Río Grande de Arecibo have sharp flood peaks associated with the period of rainband rainfall centered at 0800 UTC (Figure 4e). Storm total rainfall over much of the western portion of the island is underestimated using the tropical Z-R relationship. Widespread flooding was documented in the lower Río Arecibo Valley by *Torres-Sierra* [2002].

Figure 5. Storm total rainfall estimates (cm) for the (a) Río Canóvanas and Río Grande near el Verde, (b) Río Grande de Lóiza and Río Turabo, (c) Río Orocovis and Río Grande de Manatí, (d) Río Saliente and Río Caonillas, and (e) Río Grande de Arecibo and Río Tanamá basins (see Figure 1 for location map). The tropical Z-R relationship was used to construct rainfall estimates.

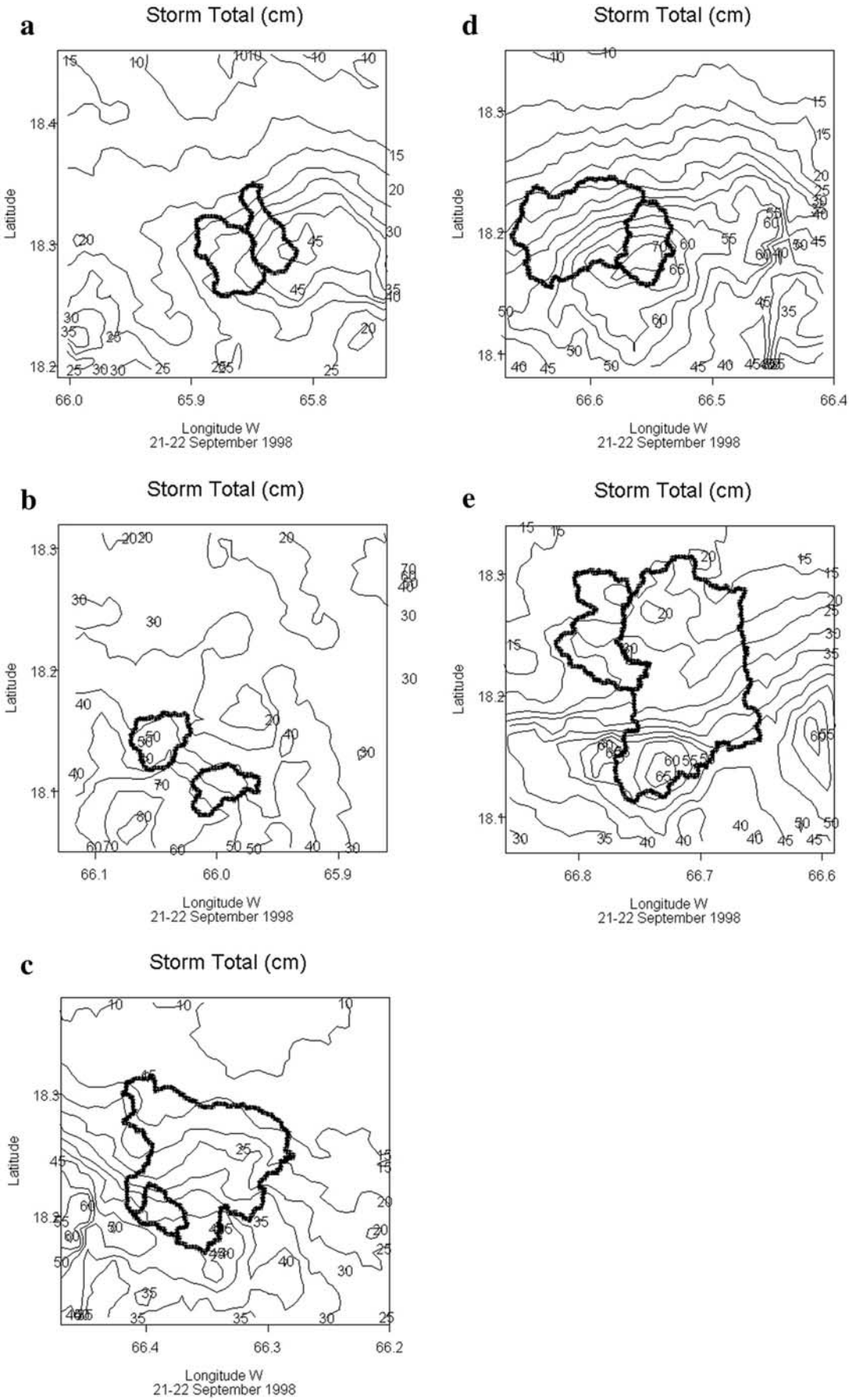
a
Storm Total (cm)
Latitude
Longitude W
21-22 September 1998
b
Storm Total (cm)
Latitude
Longitude W
21-22 September 1998
c
Storm Total (cm)
Latitude
Longitude W
21-22 September 1998
d
Storm Total (cm)
Latitude
Longitude W
21-22 September 1998
e
Storm Total (cm)
Latitude
Longitude W
21-22 September 1998

Figure 5

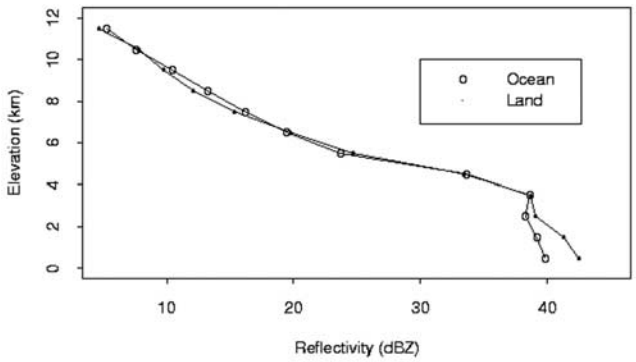

Figure 6. Mean vertical profile of reflectivity. The "ocean" profile is derived from a 30 km east-west transect 40 km south of the island. The land profile was developed from a 30 km east-west transect along the southern slopes of the island (see Figure 1).

[25] Storm total rainfall fields were computed from WSR-88D reflectivity observations for five regions, each of 900 km^2 size (Figure 5). The five regions contain the five paired watersheds used for hydrologic analyses in the following section. In each case, rainfall fields were computed using the tropical Z-R relationship with a 52 dBZ reflectivity threshold (rainfall estimates were not overly sensitive to the reflectivity threshold, based on analyses using thresholds ranging from 50 to 55 dBZ). For the Río Saliente, Manatí and Arecibo basins, analyses utilized the second tilt (1.5°) because of extensive regions of ground returns at the lowest elevation angle. For the Lóiza and Canóvanas analyses the lowest tilt was used. Ground returns were encountered at high-elevation regions. To eliminate this problem, 41 of 900 bins were removed from the Río Canóvanas analyses and 55 of 900 bins from the Lóiza analyses. For these bins, rainfall rates were interpolated from the nearest "good" bins.

[26] The largest rainfall accumulations for the storm were located along the high-elevation regions of the Río Grande de Manatí (Figure 5c), Río Saliente (Figure 5d) and Río Grande de Arecibo basins (Figure 5e). The contours of maximum rainfall from the radar rainfall analyses are oriented from southwest to northeast over the Río Saliente basin (Figure 5d), following the contours of the high-elevation maxima of the region (Figure 1). The gradients in rainfall accumulation from the center of the Río Saliente basin are much sharper to the north, with storm total rainfall decreasing from a maximum of 720 mm to a minimum of less than 500 mm at the basin outlet. An elevated region of storm total rainfall exceeding 500 mm extends southward from the Río Saliente basin. Analyses indicate a rainfall maximum extending southward from the highest elevation region of the island, with a sharp decrease in rainfall accumulation to the north of the mountain barrier.

[27] For much of the storm life cycle, the vertical structure of reflectivity in the eye wall and inner rainband region of the storm was characterized by relatively weak convection in which peak reflectivities occurred close to the radar "bright band" (the region of elevated reflectivity associated with melting snow crystals below the 0°C level). The location of the bright band was approximately 4 km above ground level. Mean vertical profiles of reflectivity were constructed for a 30 km east-west cross section located along the southern slopes of the island and a 30 km east-west cross section located 40 km south of Puerto Rico over open ocean (Figure 6). The mean reflectivity profiles are quite similar in the ice phase portion of the clouds above approximately 4 km. Below the 0°C level, there are sharp contrasts in the reflectivity profile with the lowest level reflectivity values over land nearly 1.5 dB higher than over open ocean. This difference translates into a 30% increase in rainfall over hillslopes versus over open ocean (assuming a tropical Z-R relationship). The vertical profiles are consistent with forced ascent over the upslope mountain barrier leading to high-cloud water content. Orographic enhancement of precipitation over the upslope regions of the island resulted from scavenging of high-cloud water and growth of precipitation to the ground surface. The sharp decrease in rainfall accumulation north of the mountain barrier is due to suppression of precipitation by downslope motion.

[28] Storm total rainfall estimates for the Canóvanas basin and surroundings (Figure 5a) also exhibit the striking controls of orographic precipitation mechanisms. The axis of rainfall accumulations exceeding 400 mm contains the line of highest elevation in the Luquillo (note three peaks in Figure 1). Rainfall accumulation contours ranging from 200 to 400 mm and extending northwest of the rainfall maximum, are oriented southwest to northeast, roughly following the elevation contours. The 200 mm contour in the southwestern portion of the 900 km^2 region is contained within the low-elevation valley between Canóvanas and Lóiza. The local accumulation maximum of 350 mm (see also Lóiza analyses in Figure 5b) coincides with a local topographic maximum in the valley. The major difference between rainfall accumulations in Canóvanas and the central mountain basins was tied to the contributions from the period of intense eye wall convection around 0030 UTC.

[29] The most striking aspect of Hurricane Georges (Figure 7) was the development of deep convection in the eye wall around 2300 UTC (compare with the vertical profile in Figure 6; see *Geerts et al.* [2000] for discussion of development of deep convection in Hurricane Georges over Haiti). Peak reflectivities exceeding 50 dBZ extended to 10 km AGL (Figure 7b). Development of the storm element bears marked similarities to development of the eye wall mesovortex in Hurricane Danny, as described by *Blackwell* [2000]. As this storm element passed from ocean to land from 2310 UTC to 0020 UTC on 22 September, the vertical structure of the storm changed markedly, with decreasing echo centroid elevations suggesting a transition from updraft-dominated to downdraft dominated vertical motion. Peak rainfall rates in eastern Puerto Rico were produced by the decaying phase of this element of eye wall convection.

[30] Storm total rainfall estimates for the Lóiza basin and surroundings (Figure 5b) were developed from the 0.5° elevation angle and ranged from 800 mm immediately southwest of the basin to 200 mm in the northern portion of the region. There was a sharp gradient in rainfall accumulation over the Lóiza basin, but relatively low gradients over much of the area north and east of the Lóiza basin. Storm total accumulations ranged from 700 mm at the southern boundary of the basin to 300 mm at the basin

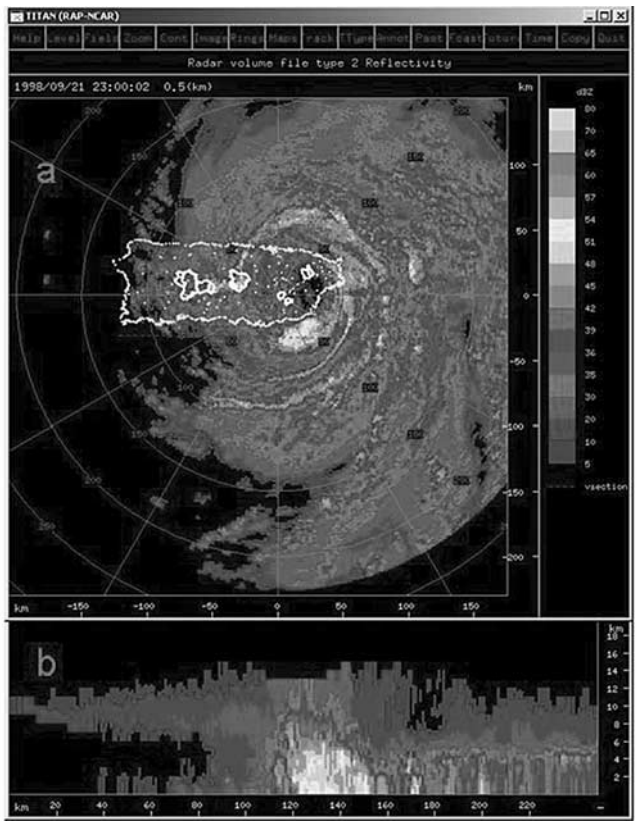

Figure 7. (a) Reflectivity image of eye wall convection at 2300 UTC on 21 September 1998 and (b) vertical profile of reflectivity at 2300 UTC along the red dashed line just south of the island of Puerto Rico in Figure 7a. See color version of this figure at back of this issue.

outlet. The local maximum in rainfall accumulation over the southern boundary of Lóiza and Turabo occurred in a region with no rain gages. The radar rainfall analyses suggest that flood peaks should have been most extreme in this region, which was the case, as discussed in the following section.

3. Flood Hydrology

[31] The preceding analyses have focused on the spatial and temporal distribution of rainfall over Puerto Rico for Hurricane Georges. The space-time rainfall distribution was linked to the structure of the hurricane and evolution of the storm structure as it passed over the island. In this section, extreme flood response for Puerto Rico is examined through analyses of rainfall and discharge observations from Hurricane Georges and through intercomparisons of flood response for Hurricane Georges with extreme flood response in the Edwards Plateau of Texas and the central Appalachian region.

[32] Because of the striking east-to-west contrasts in rainfall distribution, analyses of basin response for Hurricane Georges are carried out for a series of five paired watersheds (Table 1) extending from east to west over the island (Figure 1). The paired watersheds are (1) Río Canóvanas (USGS ID number 50061800) and Río Grande near El Verde (50064200), (2) Río Grande de Lóiza (50050900) and Río Turabo (50053025), (3) Río Orocovis (50030460) and Río Grande de Manatí near Moróvis (50031200), (4) Río Saliente (50025155) and Río Caonillas (50026025) and (5) Río Grande de Arecibo below Utuado (50024950) and Río Tanamá near Utuado (50028000). Time series plots of basin-averaged rainfall rate (derived from WSR-88D observations as described above and aggregated to 15 min time interval) and discharge (Figure 8) illustrate the contrasting rainfall distribution over the five regions and the basic elements of hydrologic response.

[33] Observed storm total accumulations over the eastern portion of the island were lower than in the central mountain region, but the highest rainfall rates were concentrated in this area. The sharp peak in rainfall rate for the two eastern rain gages (Figures 4a and 4b) was reflected in the sharp, early peaks in discharge for the Río Canóvanas and Río Grande stream gaging stations (Figure 8a). The peak discharge at the Río Grande gaging station has the second largest unit discharge flood peak for the event (30 $m^3\ s^{-1}\ km^{-2}$) (see Figure 2) and the Río Canóvanas peak (17 $m^3\ s^{-1}\ km^{-2}$) was among the largest for the event. For the 15.6 km^2 Río Grande basin, the lag time between peak rainfall rate and peak discharge was less than 30 min. For the 25.5 km^2 Río Canavanas basin, the lag time between the peak in rainfall rate and the peak discharge was less than 1 hour.

[34] The storm total runoff values for Río Grande (285 mm) and Río Canóvanas (360 mm) exceeded 90% of the storm total rainfall. Large runoff ratios in high-gradient, forested catchments are rare [*Dunne*, 1978], but have been observed in other settings. The 27 June 1995 Rapidan flood

Table 1. Station Name, USGS Identification Number, Drainage Area, and Peak Discharge for Hurricane Georges (21–22 September 1998)[a]

Name	USGS Identification	Drainage Area, km^2	Peak Discharge, $m^3\ s^{-1}\ km^{-2}$
1, Río Grande near El Verde	50064200	18.9	32.9
2, Río Canóvanas near Campo Rico	50061800	25.5	19.2
3, Río Grande de Lóiza	50050900	15.5	81.9
4, Río Turabo above Borinquen	50053025	18.5	20.1
5, Río Orocovis near Orocovis	50030460	13.0	15.1
6, Río Grande de Manatí near Morovis	50031200	55.2	6.47
7, Río Saliente at Coabey	50025155	24.0	21.8
8, Río Caonillas	50026025	98.3	10.4
9, Río Grande de Arecibo	50024950	170	12.7
10, Río Tanamá near Utuado	50029000	47.7	13.9

[a]Peak discharge is given as a unit discharge.

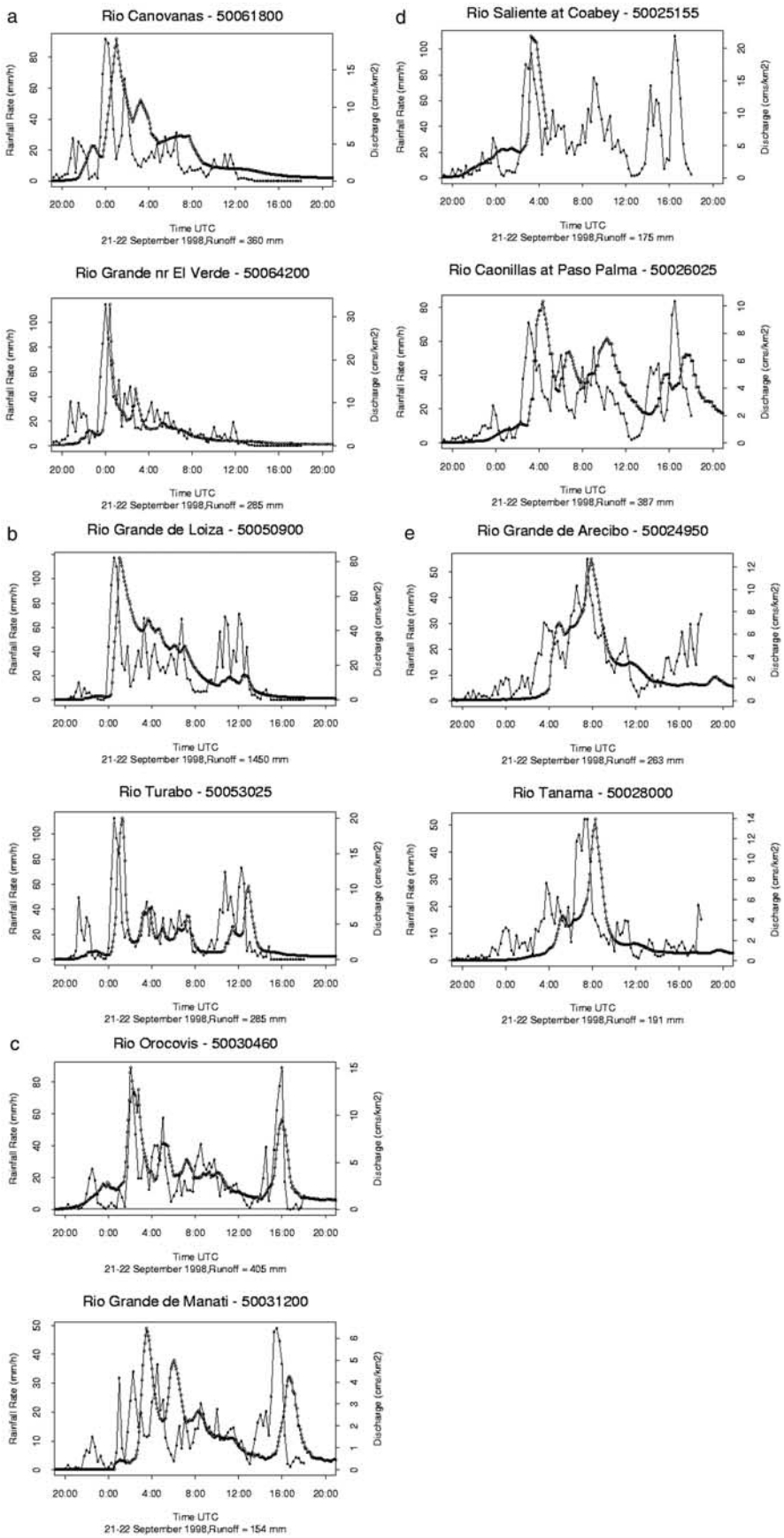

Figure 8. Time series of basin-averaged rainfall rate and discharge for (a) Río Canóvanas and Río Grande near El Verde, (b) Río Grande de Lóiza and Río Turabo, (c) Río Orocovis and Río Grande de Manatí, (d) Río Saliente and Río Caonillas, and (e) Río Grande de Arecibo and Río Tanamá.

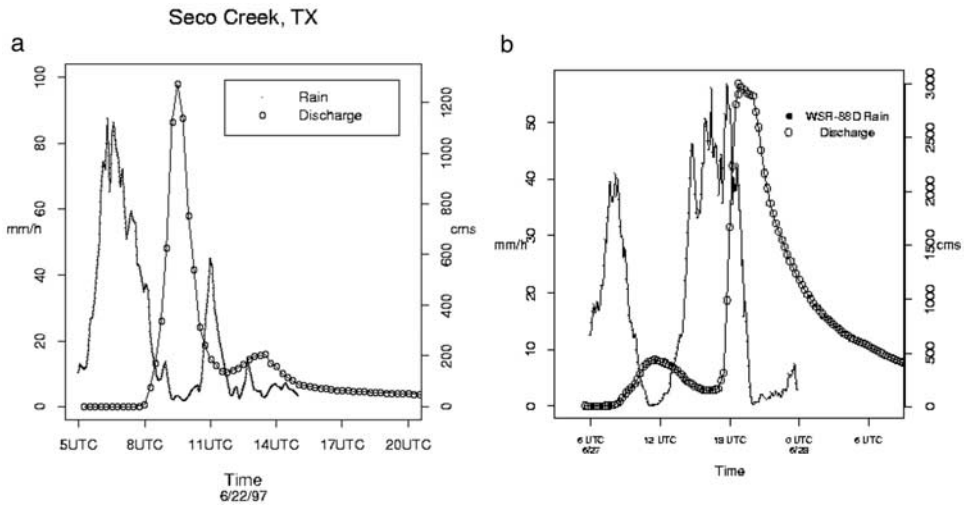

Figure 9. Time series of rainfall rate (mm h^{-1}) and discharge (m^3 s^{-1}) for the (a) 22 June 1997 Seco Creek flood on the Edwards Plateau of Texas and (b) 27 June 1995 Rapidan River flood on the east slope of the Blue Ridge in Virginia.

[*Smith et al.*, 1996] (see also Figure 9), for example, had a runoff ratio of approximately 80%.

[35] The Río Grande de Lóiza peak discharge (Figure 8b) of 81.6 m^3 s^{-1} km^{-2} was not only the largest unit discharge flood peak for the event, but also exceeds the U.S. envelope curve (Figure 2). Like the Río Grande and Río Canóvanas peaks, the Río Grande de Lóiza peak was associated with eye wall convection during the period between 2345 UTC and 0030 UTC. The most important element of the largest unit discharge flood peaks from Hurricane Georges was evolution of eye wall convection during this period.

[36] The Río Grande de Lóiza peak unit discharge of 81.6 m^3 s^{-1} km^{-2} can be expressed as a discharge rate of 300 mm h^{-1}. There is no direct support for rainfall rates approaching this magnitude, either from rain gage or radar. The storm total runoff for the Río Grande basin of 1450 mm is much larger than storm total rainfall analyses based on radar and rain gages (Figures 4 and 5). The peak discharge of the Río Turabo (the paired watershed for the Río Grande de Lóiza, see Figures 1 and 5b) was 25% of the Lóiza peak. The storm total runoff from the Lóiza basin was more than 5 times larger than the Río Turabo runoff of 285 mm. Discharge measurements for extreme flood events are subject to numerous errors [*Jarrett*, 1987; *Costa*, 1987; *Potter and Walker*, 1985; *House and Pearthree*, 1995; *Hjalmarson and Phillips*, 1997], especially those like the Río Grande de Lóiza peak for which the peak discharge estimate is obtained by a rating curve extension far beyond the largest direct discharge estimate. The 1274 m^3 s^{-1} peak discharge estimate was obtained from an extended rating curve for which the largest direct discharge measurement was 8.5 m^3 s^{-1}. Measurement error provides one possible explanation for the anomalously large discharge values for the Río Grande de Lóiza.

[37] Despite these observations, there are arguments to support the extreme nature of the Lóiza peaks. On the basis of radar observations, the upper portion of the Lóiza basin received the heaviest rainfall from the eye wall convection (Figures 4b and 4a and 5). There were no rain gages in the upper portion of the Río Grande. Radar rainfall estimates in the presence of strong downdrafts can severely underestimate rainfall rate [*Austin*, 1987; *Lee*, 1988]. Inferences about the Lóiza peak all turn on understanding the behavior of eye wall convection during the 45 min period from 2345 to 0030. Geomorphic evidence in the upper tributary basins of the Río Grande de Lóiza provides some support for high discharge peaks. Hurricane Georges rainfall and associated flooding caused numerous debris flows, channel bank erosion, and channel scour followed immediately by channel bed aggradation in some southern tributaries [*Larsen and Santiago-Román*, 2001]; there was no direct evidence, however, that debris flows directly affected the Lóiza peak). The channel bed aggradation persists as of this writing (2004) indicating continued supply of bed sediment, derived from the Hurricane Georges event.

[38] Flood peak response to Hurricane Georges was not controlled by storm total accumulation but rather by peak rainfall rates. For both the Lóiza and Río Turabo discharge observations, there are a sequence of peaks associated with rainbands from Hurricane Georges. The largest peak discharge was associated with extreme rain rates from eye wall convection and occurred early in the storm. The relative roles of peak rainfall rates and storm total accumulation have been examined by *Hewlett et al.* [1977] [see also *Dunne*, 1978].

[39] Peak discharges for the Río Orocovis and Río Grande de Manatí stream gages (Figures 8c) were also associated with eye wall convection and occurred early in the flood period. There were a series of subsequent peaks produced by the series of rainbands passing over the basin. An important aspect of these analyses, as in the Lóiza and Turabo analyses is that the flood peak response was relatively smaller for the final period of intense rainfall between 1400 and 1600 UTC than for the earlier eye wall convection. Estimated basin-averaged rainfall rates are higher for the 1400–1600 UTC period, than for the 0000–0400 UTC period, but the flood peaks are lower. These observations support the conclusion that radar-based rainfall estimates for the late periods of outer rainband

Figure 10. Boulders in the Río Saliente channel bed transported by streamflow associated with Hurricane Georges indicating high magnitude of flow. Note hat for scale. See color version of this figure at back of this issue.

convection are biased high, relative to the earlier rainfall periods. The error structure of radar rainfall estimates of hurricane rainfall vary systematically with storm structure, as described by *Molinari et al.* [1999].

[40] The Río Saliente stream gage only operated through the first peak, which was produced by rainfall from eye wall convection. The discharge record for the downstream gage at Río Caonillas exhibited five peaks, with the first peak at 0430 UTC the largest (note again the lower response to the final period of rainband rainfall). These peaks correspond to peaks in the 15 min rainfall rate time series. Storm total runoff from the Río Caonillas gage was 388 mm. Storm total runoff for the Río Salinete up until the gage ceased reporting was 175 mm. For a corresponding time period, the runoff from Río Caonillas was 95 mm, suggesting that the storm total runoff from the high-elevation region above Río Saliente was approximately 700 mm. (Figure 4d). Radar rainfall estimates for the upper Río Saliente have a closed contour of 700 mm accumulations. Radar rainfall estimates decrease to 500 mm in the vicinity of the stream gage. The magnitude of flooding in the Río Saliente is illustrated by the transport of large boulders (Figure 10).

[41] For the final pair of stream gages, the Río Tanamá and Río Grande de Arecibo, the flood peaks were produced by a period of intense rainband rainfall between 0600 and 0800 UTC. Peak discharges for these catchments were exceptionally large for their drainage area, 12 $m^3\ s^{-1}\ km^{-2}$ for the Río Grande de Arecibo, and 14 $m^3\ s^{-1}\ km^{-2}$ for the Río Tanamá. Runoff values of 263 mm for Arecibo and 191 mm for Tanamá reflect the higher rainfall accumulations in the headwaters of the Río Grande de Arecibo (Figure 5) and are consistent with the spatial distribution of rainfall. Areas of high-frequency of debris flow occurrence in the Río Grande de Arecibo basin support the inference of embedded convection that produced large rainfall rates and storm total accumulations (Figure 11).

[42] Flood response in the Río Grande de Manatí (Figure 12) is represented by the geomorphological instantaneous unit hydrograph [see *Rodriguez-Iturbe and Rinaldo*, 1997]. The GIUH, G(t), is the unit response of the drainage basin to an instantaneous pulse of runoff of unit depth, given the drainage network of the basin. We evaluate the GIUH through model analyses using a distributed hydrologic model, the Network Model [*Morrison and Smith*, 2001; *Zhang et al.*, 2001; *Giannoni et al.*, 2003; *Turner-Gillespie et al.*, 2003] that partitions the drainage basin into hillslope and channel components and represents discharge at the outlet of a drainage basin as

$$Q(t) = \int_A M\left(t - \frac{d_0(x)}{v_0} - \frac{d_1(x)}{v_1}, x\right) dx \qquad (1)$$

where Q(t) denotes discharge ($m^3\ s^{-1}$) at time t (s), A is the domain of the drainage basin, x is a point within A, $d_0(x)$ is the distance (m) from x to the channel network, v_0 is the overland flow velocity ($m\ s^{-1}$), $d_1(x)$ is the distance (m) along the channel from x to the basin outlet, v_1 is the channel flow velocity and M(t,x) is the runoff rate ($m\ s^{-1}$) at time t and location x. The total flow distance from x to the basin outlet is $d_0(x) + d_1(x)$, the sum of the overland flow distance and the channel flow distance. The runoff rate M(t,x) ($mm\ h^{-1}$) at time t and location x is computed from the rainfall rate R(t,x) using the Green-Ampt infiltration model with moisture redistribution [*Ogden and Saghafian*, 1997].

[43] The preceding formulation of basin response leads to the following representation for the GIUH:

$$G(t) \approx |A|^{-1} \int_A M_{\delta t}\left(t - \frac{d_o(x)}{v_0} - \frac{d_1(x)}{v_1}, x\right) dx \qquad (2)$$

Figure 11. Area of multiple debris flows triggered by Hurricane Georges rainfall in the Río Grande de Arecibo river basin. Vegetation scour line along channel banks and extensive reworked gravel bars in river bed are evidence of large magnitude event. Houses near river provide scale. See color version of this figure at back of this issue.

where $M_{\delta t}(t, x)$ is equal to δt^{-1} (mm h^{-1}) for t $\in (0, \delta t]$ and 0 otherwise. The expression can be simplified to

$$G(t) \approx \delta t^{-1} \frac{|A_{\delta t}(t)|}{|A|} \quad (3)$$

where

$$A_{\delta t}(t) = \left\{ x \in A : \frac{d_0(x)}{v_0} + \frac{d_1(x)}{v_1} - \delta t < t \leq \frac{d_0(x)}{v_0} + \frac{d_1(x)}{v_1} \right\} \quad (4)$$

The GIUH arises as the limit in (2) and (3) as δt decreases to 0.

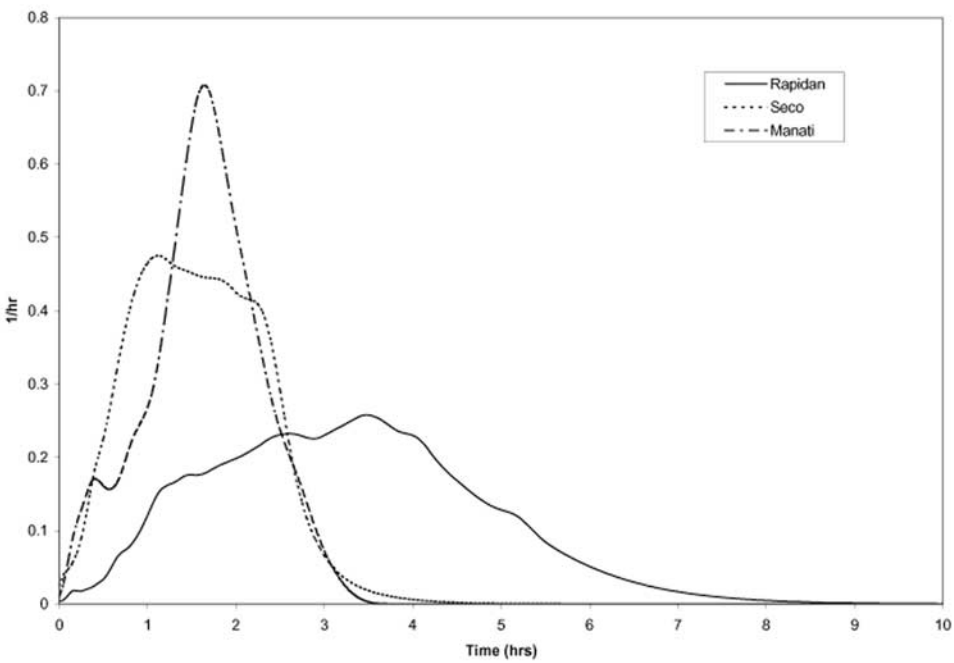

Figure 12. Geomorphological instantaneous unit hydrograph (GIUH) for Río Grande de Manatí (21 September 1998 flood), Rapidan River (27 June 1995 flood), and Seco Creek (21 June 1997 flood). In each case, GIUH represent 100 km^2 catchment area.

[44] The velocity parameters v_0 and v_1 are estimated from rainfall and discharge observations from Hurricane Georges (see *Giannoni et al.* [2001] for details). The estimated velocity parameters and the distance functions $d_0(x)$ and $d_1(x)$ derived from the extracted drainage network provide the GIUH using (2).

[45] The GIUH for the Río Grande de Manatí at 100 km^2 has a peak response at 1.1 hours. For basins with drainage area of 10 km^2, the peak time decreases to 0.2 hours. The sensitivity of Puerto Rico flood peaks to short-term (15–60 min) rainfall rates is directly tied to the characteristic response times as represented by the GIUH. Rapid response is also tied to the lack of a soil moisture deficit in Puerto Rico during the hurricane season. Generally, the annual rainfall peak is in September–October but builds during August, so that soils are at or near saturation when hurricanes hit in September. This contributes to rapid hillslope response [*Larsen and Torres-Sanchez*, 1998].

[46] The flood response of mountain watersheds in Puerto Rico is compared in Figure 12 with flood response of Seco Creek in the Edwards Plateau of Texas and the Rapidan River basin in the central Appalachian region. The 27 June 1995 Rapidan storm produced a flood peak of 10.2 m^3 s^{-1} km^{-2} at 285 km^2. The 22 June 1997 storm in the Edwards Plateau of Texas produced a flood peak of 15.7 m^3 s^{-1} km^{-2} at 117 km^2. The central Appalachians and Edwards Plateau have a history of extreme floods [*O'Connor and Costa*, 2004]. The 27 June 1995 flood peak in the Rapidan was one of the largest unit discharge flood peaks east of Mississippi River at basin scales greater than 100 km^2. The three watersheds represented in Figure 12 all have relatively large slopes, with the Rapidan slopes somewhat larger than the Río Grande de Manatí slopes and the Manatí slopes somewhat larger than the Seco Creek slopes.

[47] The GIUH for each of the three basins (Figure 12) at 100 km^2 scale was constructed from (2) using the estimated velocity parameters. To compare unit response of the drainage basins on a comparable footing it was necessary to select a common basin scale. The 100 km^2 basin represented in Figure 12 is the one for which peak model discharge occurred.

[48] The peak in the Manatí GIUH is 4 times larger than that for the Rapidan GIUH and the peak time of the Rapidan GIUH is twice as long as that of the Manatí, despite the similar slope properties of the two basins. Seco Creek has a faster, sharper GIUH than the Rapidan despite having smaller slopes. The most striking difference in the Rapidan and Manatí is between the return intervals of the two events. The 10 m^3 s^{-1} km^{-2} peak of the Rapidan flood has a return interval of more than 1000 years, while the comparable unit discharge in the Manatí has a return interval of only 20 years. The estimated return interval of the Seco Creek flood is 80 years.

[49] The extreme magnitudes of flood peaks in Puerto Rico are not solely explained by rainfall properties. The unit response of Puerto Rico basins, as represented by the GIUH, is characterized by larger flood peaks than in the Edwards Plateau and central Appalachians. Adjustment of the fluvial system to accommodate more frequent extreme rain events clearly plays a role in the magnitude and frequency of extreme floods, as discussed by *Gupta* [1988] for Caribbean islands. The GIUH results suggest that the drainage systems of regions with high frequency of extreme flood peaks are adapted to efficiently transport extreme floods. This adaptation could be in the drainage network itself, through the distribution of drainage density, through channel hydraulic geometry or through the hydraulic geometry of floodplains. The channel system may also be dynamic in the sense that flooding and mass movements create new channels and more efficient channels. River channels in many Caribbean watersheds are oversized with respect to mean annual discharge, with large, often box-shaped, incised channels, capable of transporting massive water and sediment discharge, even in headwater areas [*Gupta*, 2000; *Ahmad et al.*, 1993; *Larsen and Santiago-Román*, 2001].

4. Summary and Conclusions

[50] The interior mountain region of Puerto Rico produces some of the largest unit discharge flood peaks in the United States. Tropical cyclones are responsible for many of the extreme Puerto Rico flood peaks. Hurricane Georges produced extreme rainfall over Puerto Rico on 21–22 September 1998, resulting in a number of unit discharge flood peaks which approach or exceed the envelope curve for the conterminous United States. Examination of the hydrology and hydrometeorology of Hurricane Georges in Puerto Rico has lead to the following major conclusions.

[51] 1. The largest unit discharge flood peaks from Hurricane Georges, including the 81.6 m^3 s^{-1} km^{-2} unit discharge flood peak of the Río Grande de Lóiza, were produced by an eye wall mesovortex that intensified over open ocean and decayed with passage over the eastern edge of Puerto Rico. This storm element produced the largest measured rainfall rates at rain gage stations (160 mm h^{-1} at 15 min timescale). The transition from updraft-dominated motion over open ocean to downdraft-dominated motion over land may have played a role in the extreme rainfall rates from this storm element. The role of terrain in modifying the evolution of this storm element warrants further examination.

[52] 2. Orographic mechanisms play an important role in determining storm total accumulations in the central mountain region of Puerto Rico and in the northeastern portion of the island. Storm motion results in upslope motion on the south side of the major mountain range. Analyses of vertical reflectivity profiles suggest that upslope motion on the southern slopes of Puerto Rico amplified rainfall accumulations, relative to open ocean rainfall.

[53] 3. The conceptual model of hurricane structure, introduced by *Molinari et al.* [1999], which divides the hurricane into eye wall, inner rainband and outer rainband regions, provides a useful framework for characterizing the space-time variability of rainfall from Hurricane Georges. Important elements of storm motion include the motion of the center of circulation from east to west over Puerto Rico at approximately 21 km h^{-1}, motion of rainbands about the center of the storm circulation and motion of individual convective elements within the eye wall and rainbands.

[54] 4. Gage-radar intercomparisons for Hurricane Georges demonstrate systematic differences between the inner core region and outer core regions of the storm. Systematic overestimation of rainfall rates is characteristic

of the outer core region, using the tropical Z-R relationship. The tropical Z-R provides generally good rainfall estimates in the inner core region. Severe underestimation of rainfall rates using the tropical Z-R relationship was observed only for the eye wall mesovortex (see item 2). Underestimation in this setting is consistent with downdraft-dominated storm motion.

[55] 5. The extreme flood environment of Puerto Rico is characterized by very rapid response times. The response times are represented in terms of the GIUH, which is computed from rainfall and discharge observations. The response times of Puerto Rico catchments are rapid in comparison with extreme flood environments in the conterminous United States. In particular, the response times are short relative to the Rapidan River basin in the central Appalachians and Seco Creek in the Edwards Plateau of Texas. The GIUH analyses suggest that Puerto Rico basins are characterized by an efficient drainage network, with high drainage density and large channel capacities.

[56] 6. The response properties of Puerto Rico catchments are directly linked to the dependence of flood response on short-term rainfall rates (less than 1 hour timescale), as opposed to storm total rainfall accumulations. Peak flood response in Puerto Rico for Hurricane Georges was strongly dependent on peak 15–60 min rainfall rates and less influenced by peak storm total accumulations.

[57] **Acknowledgments.** The authors would like to acknowledge the insightful comments of John Costa. The research was supported by the National Science Foundation (NSF grants EAR-0233618, ATM-0223798, and EAR-04090502).

References

Ahmad, R., F. N. Scatena, and A. Gupta (1993), Morphology and sedimentation in Caribbean montane streams: Examples from Jamaica and Puerto Rico, *Sediment. Geol.*, *85*, 157–169.

Austin, P. M. (1987), Relation between measured radar reflectivity and surface rainfall, *Mon. Weather Rev.*, *115*, 1053–1070.

Baker, V. R. (1977), Stream channel response to floods, with examples from central Texas, *Geol. Soc. Am. Bull.*, *88*(8), 1057–1071.

Barnes, H. H., Jr., and D. B. Bogart (1961), Floods of September 6, 1960, in eastern Puerto Rico, *U.S. Geol. Surv. Circ.*, *451*, 13 pp.

Barry, R. G. (1992), *Mountain Weather and Climate*, 402 pp., Routledge, Boca Raton, Fla.

Bender, M. A. (1997), The effect of relative flow on the asymmetric structure in the interior of hurricanes, *J. Atmos. Sci.*, *54*, 703–724.

Bender, M. A., R. E. Tulyea, and Y. Kurihara (1987), A numerical study of the effect of island terrain on tropical cyclones, *Mon. Weather Rev.*, *115*, 130–155.

Blackwell, K. G. (2000), Evolution of Hurricane Danny at landfall: Doppler-observed eyewall replacement, vortex contraction/intensification and low-level wind maxima, *Mon. Weather Rev.*, *128*, 4002–4016.

Calvesbert, R. J. (1970), Climate of Puerto Rico and the U.S. Virgin Islands, in *Climatography of the U.S.*, *Rep. 60-52*, 28 pp., U.S. Dep. of Comm., Washington, D. C.

Cecil, D. J., E. J. Zipser, and S. W. Nesbitt (2002), Reflectivity, ice scattering and lightning characteristics of hurricane eyewalls and rainbands, part 1: Quantitative description, *Mon. Weather Rev.*, *130*, 769–784.

Costa, J. E. (1987), Hydraulics and basin morphometry of the largest flash floods in the conterminous United States, *J. Hydrol.*, *93*(3–4), 313–338.

Dunne, T. E. (1978), Field studies of hillslope flow processes, in *Hillslope Hydrology*, pp. 227–293, John Wiley, Hoboken, N. J.

Enzel, Y., L. L. Ely, P. K. House, V. R. Baker, and R. H. Webb (1993), Paleoflood evidence for a natural upper bound to flood magnitudes in the Colorado River basin, *Water Resour. Res.*, *29*(7), 2287–2297.

Fulton, R. A., J. P. Breidenbach, D.-J. Seo, D. A. Miller, and T. O'Bannon (1998), The WSR-88D rainfall algorithm, *Weather Forecasting*, *13*, 377–395.

Geerts, B., G. M. Heymsfield, L. Tian, J. B. Halverson, A. Guillory, and M. I. Mejia (2000), Hurricane George's landfall in the Dominican Republic: Detailed airborne Doppler imagery, *Bull. Am. Meteorol. Soc.*, *81*(5), 999–1018.

Giannoni, F., J. A. Smith, Y. Zhang, and G. Roth (2003), Hydrologic modeling of extreme floods using radar rainfall estimates, *Adv. Water Resour.*, *26*, 195–2003.

Gupta, A. V. (1988), Large floods as geomorphic events in the humid tropics, in *Flood Geomorphology*, edited by V. R. Baker, R. C. Kochel, and P. C. Patton, pp. 301–315, John Wiley, Hoboken, N. J.

Gupta, A. (2000), Hurricane floods as extreme geomorphic events, in *The Hydrology-Geomorphology Interface: Rainfall, Floods, Sedimentation, Land Use*, edited by M. A. Hasan, O. Slaymaker, and S. M. Berkowicz, *IAHS Publ.*, *261*, 215–228.

Hewlett, J. D., J. D. Fortson, and G. B. Cunningham (1977), The effect of rainfall intensity on storm flow and peak discharge from forest land, *Water Resour. Res.*, *13*(2), 259–266.

Hjalmarson, H. W., and J. V. Phillips (1997), Potential effects of translatory waves on estimation of peak flows, *J. Hydraul. Eng.*, *123*(6), 571–575.

House, P. K., and P. A. Pearthree (1995), A geomorphologic and hydrologic evaluation of an extraordinary flood discharge estimate: Bronco Creek, Arizona, *Water Resour. Res.*, *31*(12), 3059–3073.

Houze, R. A. (1993), *Cloud Dynamics*, 570 pp., Elsevier, New York.

Jarrett, R. D. (1987), Errors in slope-area computations of peak discharge in mountain streams, *J. Hydrol.*, *96*(1–4), 53–67.

Jorgensen, D. A., E. J. Zipser, and M. A. Lemone (1985), Vertical motion in intense hurricanes, *J. Atmos. Sci.*, *42*, 839–856.

Larsen, M. C., and A. Santiago-Román (2001), Mass wasting and sediment storage in a small montane watershed: An extreme case of anthropogenic disturbance in the humid tropics, in *Geomorphic Processes and Riverine Habitat*, *Water Sci. Appl.*, vol. 4, edited by J. M. Dorava et al., pp. 119–138, AGU, Washington, D. C.

Larsen, M. C., and A. Simon (1993), Rainfall-threshold conditions for landslides in a humid-tropical system, Puerto Rico, *Geogr. Ann.*, *75A*(1–2), 13–23.

Larsen, M. C., and A. J. Torres-Sanchez (1998), The frequency and distribution of recent landslides in three montane tropical regions of Puerto Rico, *Geomorphology*, *24*, 309–331.

Lee, A. C. (1988), The influence of vertical air velocity on the remote microwave measurement of rain, *J. Atmos. Oceanic Technol.*, *5*, 727–735.

Marks, F. D. (1985), Evolution of the structure of precipitation in hurricane Allen (1980), *Mon. Weather Rev.*, *113*, 909–930.

Marks, F. D., and R. A. Houze (1987), Inner core structure of hurricane Alicia from airborne Doppler radar observations, *J. Atmos. Sci.*, *44*, 1296–1317.

Michaud, J. D., K. K. Hirschboeck, and M. Winchell (2001), Regional variation in small-basin floods in the United States, *Water Resour. Res.*, *37*(5), 1405–1416.

Molinari, J., P. Moore, and V. Idone (1999), Convective structure of hurricanes as revealed by lightning locations, *Mon. Weather Rev.*, *127*, 520–534.

Morrison, J. E., and J. A. Smith (2001), Scaling properties of flood peaks, *Extremes*, *4*(1), 5–23.

O'Connor, J. E., and J. E. Costa (2004), Spatial distribution of the largest rainfall-runoff floods from basins between 2.6 and 26,000 km^2 in the United States and Puerto Rico, *Water Resour. Res.*, *40*, W01107, doi:10.1029/2003WR002247.

Ogden, F. L., and B. Saghafian (1997), Green and ampt infiltration with redistribution, *J. Irrig. Drain. Eng.*, *123*(5), 386–393.

Osterkamp, W. R., and J. M. Friedman (2000), The disparity between extreme rainfall events and rare floods with emphasis on the semi-arid American West, *Hydrol. Processes*, *14*(16–17), 2817–2829.

Potter, K. W., and J. T. Walker (1985), An empirical study of flood measurement error, *Water Resour. Res.*, *21*(3), 403–406.

Rodriquez-Iturbe, I., and A. Rinaldo (1997), *Fractal River Basins*, 547 pp., Cambridge Univ. Press, Cambridge, Mass.

Scatena, F. N., and M. C. Larsen (1991), Physical aspects of Hurricane Hugo in Puerto Rico, *Biotropica*, *23*(4A), 317–323.

Smith, J. A., M. L. Baeck, M. Steiner, and A. J. Miller (1996), Catastrophic rainfall from an upslope thunderstorm in the central Appalachians: The Rapidan storm of June 27, 1995, *Water Resour. Res.*, *32*(10), 3099–3113.

Smith, J. A., M. L. Baeck, J. E. Morrison, and P. Sturdevant-Rees (2000), Catastrophic rainfall and flooding in Texas, *J. Hydrometeorol.*, *1*(1), 5–25.

Smith, R. B., and D. F. Smith (1995), Pseudoinviscid wake formation by mountains in shallow-water flow with a drifting vortex, *J. Atmos. Sci.*, *52*, 436–454.

Sturdevant-Rees, P. L., J. A. Smith, J. E. Morrison, and M. L. Baeck (2001), Tropical storms and the flood hydrology of the central Appalachians, *Water Resour. Res.*, *37*(8), 2143–2168.

Torres-Sierra, H. (1997), Hurricane Hortense impact on surface water in Puerto Rico, *U.S. Geol. Surv. Fact Sheet*, *FS-014-97*, 4 pp.

Torres-Sierra, H. (2002), Flood of September 22, 1998, in Arecibo and Utuado, Puerto Rico, *U.S. Geol. Surv. Water Resour. Invest. Rep.*, *01-4247*.

Turner-Gillespie, D. F., J. A. Smith, and P. D. Bates (2003), Attenuating reaches and the regional flood response of an urbanizing drainage basin, *Adv. Water Resour.*, *26*, 673–684.

U.S. Geological Survey (1999), Puerto Rico, *U.S. Geol. Surv. Fact Sheet, FS-040-99*, 4 pp. (Available at http://water.usgs.gov/pubs/fs/FS-040-99/pdf/fs-040-99.pdf)

Willoughby, H. E., F. D. Marks, and R. J. Feinberg (1984), Stationary and moving convective bands in hurricanes, *J. Atmos. Sci.*, *41*, 3189–3211.

Zhang, Y., J. A. Smith, and M. L. Baeck (2001), The hydrology and hydrometeorology of extreme floods in the Great Plains of eastern Nebraska, *Adv. Water Resour.*, *24*, 1037–1050.

M. L. Baeck and J. A. Smith, Department of Civil and Environmental Engineering, Princeton University, Princeton, NJ 08544, USA. (jsmith@princeton.edu)

M. C. Larsen, U.S. Geological Survey, Reston, VA 20192, USA.

P. Sturdevant-Rees, Department of Civil and Environmental Engineering, University of Massachusetts, Amherst, MA 01003-5205, USA.

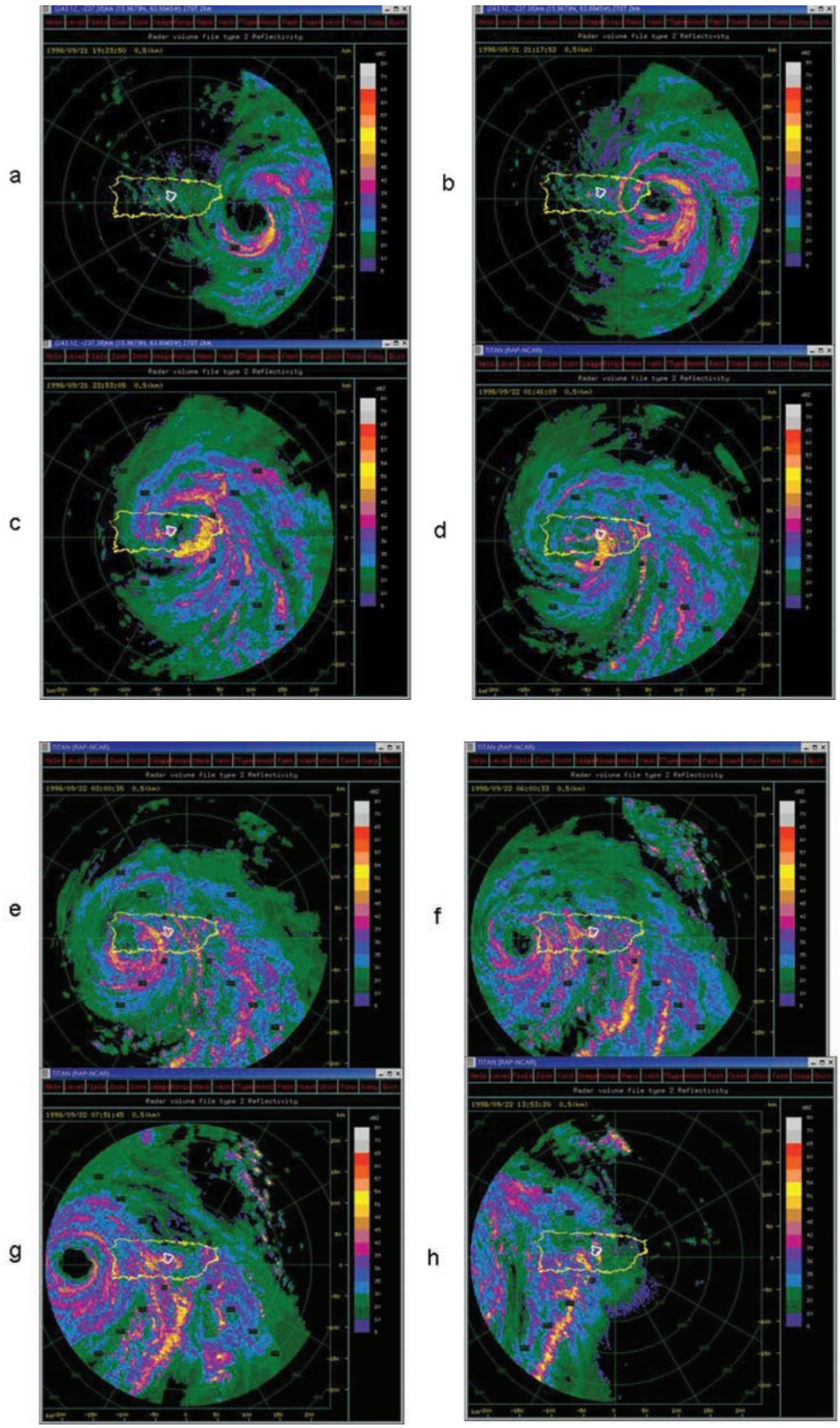

Figure 3. Reflectivity images from the San Juan, Puerto Rico, WSR-88D (lowest elevation angle) for 21 September 1998 at (a) 1923 UTC (b) 2117 UTC, and (c) 2353 UTC and for 22 September 1998 at (d) 0141 UTC (e) 0300 UTC, (f) 0600 UTC, (g) 0751 UTC and (h) 1353 UTC. Puerto Rico is outlined in yellow and the Río Grande de Manatí basin boundary is outlined in white.

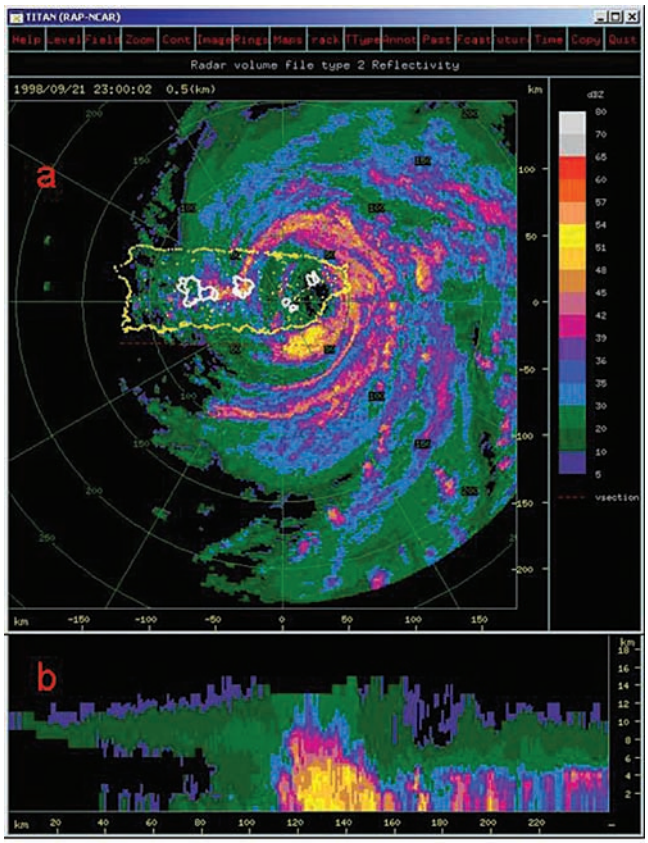

Figure 7. (a) Reflectivity image of eye wall convection at 2300 UTC on 21 September 1998 and (b) vertical profile of reflectivity at 2300 UTC along the red dashed line just south of the island of Puerto Rico in Figure 7a.

Figure 10. Boulders in the Río Saliente channel bed transported by streamflow associated with Hurricane Georges indicating high magnitude of flow. Note hat for scale.

Figure 11. Area of multiple debris flows triggered by Hurricane Georges rainfall in the Río Grande de Arecibo river basin. Vegetation scour line along channel banks and extensive reworked gravel bars in river bed are evidence of large magnitude event. Houses near river provide scale.